Chemistry of C-Trimethylsilyl-Substituted Heterocarboranes. 30. Synthetic and Structural Studies on Oxide Ion Encapsulating Tetralanthanide Tetrahedra Surrounded by "Carbons Apart" C_2B_4-Carborane Ligands (Ln(III) = La, Nd, Gd, Tb, Ho, Lu)

Jianhui Wang, Shoujian Li, Chong Zheng, Ang Li, and Narayan S. Hosmane*

Department of Chemistry and Biochemistry, Northern Illinois University, DeKalb, Illinois 60115

John A. Maguire

Department of Chemistry, Southern Methodist University, Dallas, Texas 75275

Herbert W. Roesky

Institut für Anorganische Chemie, Universität Göttingen, D-37077 Göttingen, Germany

Christopher C. Cummins

Department of Chemistry, Massachusetts Institute of Technology, Cambridge, Massachusetts 02139

Wolfgang Kaim

Institut für Anorganische Chemie, Universität Stuttgart, D-70550 Stuttgart, Germany

Received May 27, 2004

The reactions of *closo-exo*-5,6-Na(THF)$_2$-1-Na(THF)$_2$-2,4-(SiMe$_3$)$_2$-2,4-$C_2B_4H_4$ (**1**) with anhydrous $LnCl_3$ (Ln = La, Nd, Gd, Tb, Ho, Lu) and freshly distilled H_2O in molar ratios of 5:4:1 gave crystalline solids, identified as the new oxolanthanacarboranes {[η^5-1-Ln(THF)$_n$-2,4-(SiMe$_3$)$_2$-2,4-$C_2B_4H_4$]$_4$(μ-Cl)$_2$(μ_4-O)}·*y*THF (Ln = La (**2**), *n* = 0, *y* = 1; Ln = Nd (**3**), *n* = 1, *y* = 0; Ln = Gd (**4**), *n* = 0, *y* = 1; Ln = Tb (**5**), *n* = 1, *y* = 0; Ln = Ho (**6**), *n* = 0, *y* = 1; Ln = Lu (**7**), *n* = 1, *y* = 0), in 73−86% yields. All new compounds were characterized by IR spectroscopy and elemental analyses. While the diamagnetic compounds **2** and **7** were also studied by ^{1}H, ^{13}C, and ^{11}B NMR spectroscopy, the lanthanacarboranes **3** and **5**−**7** were further characterized by single-crystal X-ray diffraction analyses. The species **3**, **5**, and **7** were found to be isostructural, all containing oxide ion encapsulating tetralanthanide cores, Ln(μ_4-O), that are stabilized by coordinating two carborane ligands: one in an η^5 fashion via the C_2B_3-bonding face and the other via two Ln−H−B bridges to a neighboring cage. Complexes **3** and **5**−**7** crystallized in the monoclinic space group *C*2/*c* with *a* = 23.748(5), 23.577(5), 28.403(5), and 23.544(5) Å, *b* = 18.632(5), 18.513(5), 12.835(2), and 18.440(5) Å, *c* = 22.798(5), 22.602(5), 27.879(5), and 22.480(5) Å, β = 104.338(5), 104.092(5), 117.820(3), and 104.153(5)°, and *V* = 9774(64), 9568(4), 8989(13), and 9464(4) Å^3, respectively (*Z* = 4). The final refinements of **3** and **5**−**7** converged at R1 = 0.0795, 0.0703, 0.0367, and 0.0904; *w*R2 =0.1793, 0.1686, 0.794, and 0.1844, and GOF = 1.401, 1.305, 1.446, and 1.498, respectively. The room-temperature magnetic susceptibility of the holmium compound **6** was found to be 10.3 μ_B per lanthanide metal.

Introduction

A large number of studies has been directed toward the interaction between organic compounds and metal oxides, prompted by the fact that numerous catalytic processes involve such interactions.[1] Organometallic oxides, such as alkoxo- and aryloxolanthanides of the form Ln(OR)$_3$,[3] can serve as useful models for that approach.[2] In many cases these compounds, as well as their monocyclopentadienyl analogues, have complex oligomeric structures, which are often stabilized by interstitial anions such as an oxide, O^{2-}.[4−6] The oxide ion can link three to six lanthanide metal atoms, forming a metal−oxide cluster core.[2−7] The metals can also be complexed by various organic ligands. Our interest in oxolanthanide compounds stems from the

* To whom correspondence should be addressed. E-mail: nhosmane@niu.edu.

10.1021/om0496176 CCC: $27.50
Publication on Web 08/21/2004

observation that, unlike the larger cage (C_2B_9 and C_2B_{10}) analogues, the small-cage carboranes can form unusual oxolanthanacarboranes of the type {[η^5-1-Ln-2,3-$(SiMe_3)_2$-2,3-$C_2B_4H_4$]$_3$[(μ-1-Li-2,3-$(SiMe_3)_2$-2,3-$C_2B_4H_4$)$_3$(μ_3-OMe)]-[μ-Li(THF)]$_3$(μ_3-O)} (Ln = Nd, Sm, Gd, Tb, Dy, Ho).[8] These compounds were the unexpected products of reactions between 2 equiv of the THF-solvated dilithium compound of [2,3-$(SiMe_3)_2C_2B_4H_4]^{2-}$ and anhydrous $LnCl_3$ in solvent mixtures of dry benzene and THF. Although the mechanism of these reactions is not known, it may involve the initial formation of the respective half-sandwich lanthanacarborane, which then reacts with the remaining lithiacarborane precursor in the presence of degradation products of the THF solvent to yield the corresponding trinuclear oxo−Ln(III)−carborane clusters. Support for this sequence was found in the report of the formation of a monomeric half-sandwich samaracarborane, {1,1-(t-$C_4H_9OH)_2$-1-(t-C_4H_9-O)-2,3-$(SiMe_3)_2$-4,5-[Li(THF)Cl]-*closo*-η^5-1-Sm-2,3-C_2B_4-H_4}·THF.[9] In addition, when TMEDA was substituted for THF, the course of the reactions was quite different in that the expected full-sandwich lanthanacarboranes [Li(TMEDA)$_2$][1-Cl-1-(μ-Cl)-2,2′,3,3′-$(SiMe_3)_4$-5,6-[(μ-H)$_2$Li-(TMEDA)]-4,4′,5′-[(μ-H)$_3$Li(TMEDA)]-1,1′-Ln(2,3-$C_2B_4H_4)_2$] were the only detectable products.[10] It should be noted that only the "carbons adjacent" (2,3-C_2B_4) carboranes seem to show this sensitivity to solvent variation; the analogous "carbons apart" (2,4-C_2B_4) isomers,[11] as well as the larger cage (C_2B_9) carboranes,[12] gave only the simpler full- and half-sandwich lanthanacarboranes. The use of THF as an oxygen source in the syntheses of the trinuclear oxolanthanacarboranes has several disadvantages. It greatly complicates the development of any general synthetic scheme, it is difficult to control the stoichiometry of the synthesis, and it introduces a number of other degradation products such as MeO^- that can then influence the reaction. These complexities led us to question whether there could be alternative methods to synthesize oxolanthanacarboranes routinely. In a preliminary communication, we have reported a more direct synthetic approach and the crystal structure of the oxide ion encapsulating tetraholmium tetrahedron that is complexed with small-cage "carbons apart" C_2B_4-carborane ligands.[13] In this report we demonstrate that this synthetic method is a general one that can be applied to produce a number of oxo organometallics of the lanthanide metals, involving a variety of π-complexing small-cage carborane ligands. Herein, we report the details of these investigations.

Experimental Section

Materials. All manipulations were carried out either under a dry argon atmosphere or on a high-vacuum line. Benzene, tetrahydrofuran (THF), and *n*-hexane were dried over NaH or Na/benzophenone and doubly distilled before use. All other solvents were dried over 4−8 Å mesh molecular sieves (Aldrich) and were either saturated with dry argon or degassed before use. H_2O/THF solutions of the lanthanide reagents were prepared by dissolving the stoichiometric amounts of freshly distilled water into dry THF containing $LnCl_3$. The synthesis of *closo-exo*-5,6-Na(THF)$_2$-1-Na(THF)$_2$-2,4-$(SiMe_3)_2$-2,4-$C_2B_4H_4$ followed the literature procedure.[14] Prior to use, $LaCl_3$, $NdCl_3$, $GdCl_3$, $TbCl_3$, $HoCl_3$, and $LuCl_3$ (Aldrich) were degassed in vacuo at 130 °C for 24 h.

Spectroscopic Procedures. Proton, boron-11, and carbon-13 NMR spectra were recorded on a Bruker Fourier transform multinuclear NMR spectrometer at 200, 64.2, and 50.3 MHz, respectively. Infrared spectra were recorded on a Perkin-Elmer Model 1600 FT-IR spectrophotometer and Nicolet Magna 550 FT-IR spectrophotometer. Elemental analyses were determined in house at Northern Illinois University using a Perkin-Elmer 2400 CHN elemental analyzer.

Magnetic Susceptibility. Magnetic susceptibilities were measured with a MPMS Quantum Design SQUID magnetometer between 5 K and room temperature in a magnetic field of 1 T. The samples (~20 mg) were contained in gelatin capsules,[15] the magnetization of which was determined in separate runs and subtracted. Corrections for core diamagnetism were not applied.

Computational Details. Density functional theory (DFT) calculations were carried out on the model compound La_4OCl_2-(2,4-$C_2B_4H_6)_4(OH_2)_4$ using the Amsterdam Density functional program package,[16,17] version 2002.03.[18] The local exchange-correlation potential of Vosko et al.[19] (VWN) was augmented self-consistently with gradient-corrected functionals for electron exchange according to Becke[20] and electron correlation according to Perdew.[21] Relativistic effects were included using

(1) (a) Rao, C. N. R.; Raveau, B. *Transition Metal Oxides*; VCH: Weinheim, Germany, 1995. (b) Thomas, J. M.; Thomas, W. J. *Principles and Practice of Heterogeneous Catalysis*; VCH: Weinheim, Germany, 1997. (c) Ertl, G.; Knözinger, H.; Weitkamp, J. *Handbook of Heterogeneous Catalysis*; VCH: Weinheim, Germany, 1997.

(2) (a) Cornils, B.; Herrmann, W. A. *Applied Homogeneous Catalysis with Organometallic Compounds*; VCH: Weinheim, Germany, 1996. (b) Basset, J.-M.; Gates, B. C.; Candy, J. P.; Choplin, A.; Leconte, M.; Quignard, F.; Santini, C. *Surface Organometallic Chemistry: Molecular Approaches to Surface Catalysis*; Kluwer: Dordrecht, The Netherlands, 1988. (c) Basset, J.-M.; Candy, J. P.; Choplin, A.; Didillon, B.; Quignard, F.; Théolier, A. In *Perspectives in Catalysis*; Thomas, J. P., Zamaraev, K., Eds.; Blackwell: Oxford, U.K., 1991; pp 125−145.

(3) Mehrotra, R. C.; Singh, A.; Tripathi, U. M. *Chem. Rev.* **1991**, *91*, 1287−1303.

(4) Evans, W. J.; Sollberger, M. S.; Hanusa, T. P. *J. Am. Chem. Soc.* **1988**, *110*, 1841−1850.

(5) (a) Evans, W. J.; Sollberger, M. S. *J. Am. Chem. Soc.* **1986**, *108*, 6095−6096. (b) Evans, W. J.; Sollberger, M. S.; Shreeve, J. L.; Olofson, J. M.; Hain, J. H., Jr.; Ziller, J. W. *Inorg. Chem.* **1992**, *31*, 2492−2501.

(6) (a) Schumann, H.; Kociok-Köhn, G.; Loebel, Z. *Anorg. Allg. Chem.* **1990**, *581*, 69−81. (b) Yunlu, K.; Gradeff, P. S.; Edelstein, N.; Kot, W.; Shalimoff, G.; Streib, W. E.; Vaartstra, B. A.; Caulton, K. G. *Inorg. Chem.* **1991**, *30*, 2317−2321.

(7) Schumann, H.; Meese-Marktscheffel, J. A.; Esser, L. *Chem. Rev.* **1995**, *95*, 865−986 and references therein.

(8) (a) Hosmane, N. S.; Wang, Y.; Oki, A. R.; Zhang, H.; Maguire, J. A. *Organometallics* **1996**, *15*, 626−638. (b) Zheng, C.; Hosmane, N. S.; Zhang, H.; Zhu, D.; Maguire, J. A. *Internet J. Chem.* **1999**, *2*, 10 (URL: http://www.ijc.com/articles/1999v2/10/).

(9) Hosmane, N. S.; Oki, A. R.; Zhang, H. *Inorg. Chem. Commun.* **1998**, *1*, 101−104.

(10) Hosmane, N. S.; Wang, Y.; Zhang, H.; Maguire, J. A.; McInnis, M.; Gray, T. G.; Collins, J. D.; Kremer, R. K.; Binder, H.; Waldhör, E.; Kaim, W. *Organometallics* **1996**, *15*, 1006−1013.

(11) (a) Hosmane, N. S.; Li, S.-J.; Zheng, C.; Maguire, J. A. *Inorg. Chem. Commun.* **2001**, *4*, 104−107. (b) Wang, J.; Li, S.-J.; Zheng, C.; Maguire, J. A.; Hosmane, N. S. *Organometallics* **2002**, *21*, 3314−3316.

(12) Manning, M. J.; Knobler, C. B.; Hawthorne, M. F. *J. Am. Chem. Soc.* **1988**, *110*, 4458−4459.

(13) Wang, J.; Li, S.-J.; Zheng, C.; Hosmane, N. S.; Maguire, J. A.; Roesky, H. W.; Cummins, C. C.; Kaim, W. *Organometallics* **2003**, *22*, 4390−4392.

(14) Hosmane, N. S.; Jia, L.; Zhang, H.; Bausch, J. W.; Prakash, G. K. S.; Williams, R. E.; Onak, T. P. *Inorg, Chem.* **1991**, *30*, 3793−3795.

(15) Commercially available pharmaceutical gelatin capsules.

(16) te Velde, G.; Bickelhaupt, F. M.; van Gisbergen, S. J. A.; Fonseca Guerra, C.; Baerends, E. J.; Snijders, J. G.; Ziegler, T. *J. Comput. Chem.* **2001**, *22*, 931−967.

(17) Fonseca-Guerra, C.; Snijders, J. G.; te Velde, G.; Baerends, E. J. *Theor. Chem. Acc.* **1998**, *99*, 391−403.

(18) ADF2002.03; SCM, Theoretical Chemistry, Vrije Universiteit, Amsterdam, The Netherlands (http://www.scm.com).

(19) Vosko, S. H.; Wilk, L.; Nusair, M. *Can. J. Phys.* **1980**, *58*, 1200.

(20) Becke, A. *Phys. Rev. A* **1988**, *38*, 3098.

(21) (a) Perdew, J. P. *Phys. Rev. B* **1986**, *34*, 7406. (b) Perdew, J. P. *Phys. Rev. B* **1986**, *33*, 8822−8824.

the zero-order regular approximation (ZORA).[22] The basis set used was the all-electron ADF ZORA/TZ2P (triple-ζ with two polarization functions) basis. The initial geometry of the model compound was based on the crystallographically determined structure of $Nd_4OCl_2(C_2B_4H_4[SiMe_3]_2)_4(THF)_4$. The optimized structure of $La_4OCl_2(2,4\text{-}C_2B_4H_6)_4(OH_2)_4$ along with some selected interatomic distances are given in the Supporting Information.

Data for plots of the electron localization function (ELF) were generated by postprocessing an ADF calculation using the DGRID/BASIN program[23] and plotted using GNUPLOT.[24]

Synthetic Procedures. All experiments were carried out in 100 mL Pyrex glass round-bottom flasks equipped with magnetic stirring bars and high-vacuum Teflon valves. After their initial purifications, nonvolatile substances were manipulated in either a drybox or a glovebag, under an atmosphere of dry nitrogen or argon. All known compounds were verified by comparing their IR and/or ^{1}H NMR spectra with those of authentic samples.

Synthesis of {[η^5-1-La-2,4-$(SiMe_3)_2$-2,4-$C_2B_4H_4$]$_4$(μ-Cl)$_2$(μ_4-O)}·THF (2). A 0.50 g (2.04 mmol) sample of anhydrous $LaCl_3$ was added to dry THF (20 mL) under argon, and the resulting heterogeneous mixture was stirred overnight. This mixture was cooled to −78 °C, and then 0.0092 g (0.51 mmol) of H_2O in 5 mL of THF was added dropwise with constant stirring over a period of 10 min. The resulting mixture was slowly warmed to room temperature and stirred for 4 h at this temperature. At this point, the temperature of the reaction mixture was increased to 60 °C with constant stirring over another 12 h period until a homogeneous solution was obtained. The solution was cooled to −78 °C, and to this was added slowly in vacuo 1.44 g (2.55 mmol) of *closo-exo*-5,6-Na(THF)$_2$-1-Na(THF)$_2$-2,4-$(SiMe_3)_2$-2,4-$C_2B_4H_4$ (**1**) in 20 mL of THF. The resulting reaction mixture, containing a 5:4:1 molar ratio of **1** to $LaCl_3$ to H_2O, was warmed slowly to room temperature with constant stirring. After 4 h of stirring, the reaction mixture was refluxed for 24 h at 70 °C, during which time the heterogeneous mixture turned pale yellow. This product mixture was then filtered through a glass frit in vacuo to collect a clear yellow filtrate. The solid remaining on the frit was extracted repeatedly with anhydrous benzene, and the resulting off-white residue, identified as NaCl, was discarded. The combined filtrates and the benzene extracts were pooled and the solvents removed in vacuo to obtain a yellow solid. The solid was then washed repeatedly with *n*-hexane to collect a pale yellow powder, identified as {[η^5-1-La-2,4-$(SiMe_3)_2$-2,4-$C_2B_4H_4$]$_4$(μ-Cl)$_2$(μ_4-O)}·THF (**2**; 0.60 g, 0.38 mmol; mp > 250 °C dec; soluble in polar solvents and sparingly soluble in *n*-hexane), which was recovered in 75% yield. Anal. Calcd (found) for $C_{32}H_{88}B_{16}Cl_2La_4OSi_8$·THF: C, 27.28 (27.64); H, 6.10 (5.91). IR (cm^{-1}, KBr pellet): 2948 (s), 2887 (m), 2507 (br, s) [ν(B−H)], 2463 (br, s) [ν(B−H)], 1396 (s), 1240 (s), 1194 (w) 1172 (w), 1106 (br, m) 1048 (s), 832 (vs), 746 (m), 681 (m), 626 (m); NMR data for compound **2**: ^{1}H NMR (d_8-THF, external Me_4Si) δ 0.01 [36H, s, −Si(CH_3)$_3$], 0.18 [36H, s, −Si(CH_3)$_3$], 1.73 [4H, m, THF, $J(^1H-^1H)$ = 3.37 Hz], 3.58 [4H, m, THF, $J(^1H-^1H)$ = 3.37 Hz]; ^{13}C NMR (d^8-THF, external Me_4Si) δ 0.294 [Si(CH_3)$_3$], 22.85 [C_4H_8O], 64.56 [C_4H_8O], 101.28 [Si-$C_{(cage)}$]; ^{11}B NMR (d_8-THF, relative to external BF_3·OEt_2) δ 23.07 (br), 1.98 [br, basal *B*H], −33.94 [br], −52.21 [d, apical *B*H, $^1J(^{11}B-^1H)$ = 159 Hz].

Synthesis of {[η^5-1-Nd(THF)-2,4-$(SiMe_3)_2$-2,4-$C_2B_4H_4$]$_4$(μ-Cl)$_2$(μ_4-O)} (3). This compound was prepared as blue crystals from the reaction of *closo-exo*-5,6-Na(THF)$_2$-1-Na(THF)$_2$-2,4-$(SiMe_3)_2$-2,4-$C_2B_4H_4$ (**1**; 1.41 g, 2.50 mmol), anhydrous $NdCl_3$ (0.50 g, 2.00 mmol), and H_2O (0.0090 g, 0.50 mmol) in a molar ratio of 5:4:1 in 30 mL of dry THF, using a procedure similar to that described in the synthesis of **2**, except that the powdered product was further recrystallized in anhydrous benzene. Yield: 0.71 g, 0.39 mmol (78%). Anal. Calcd (found) for $C_{48}H_{120}B_{16}Cl_2Nd_4O_5Si_8$ (**3**): C, 31.63 (31.58); H, 6.63 (6.32). IR (cm^{-1}, KBr pellet): 2951 (s), 2887 (m), 2536 (m) [ν(B−H)], 2498 (s, s) [ν(B−H)], 2428 (s, s) [ν(B−H)], 2376 (s, w) [ν(B−H)], 1398 (s), 1240 (s), 1177 (w) 1140 (w), 1111 (w), 1021(s), 840 (vs), 758 (m), 688 (m), 627 (m). No useful NMR spectra could be obtained.

Synthesis of {[η^5-1-Gd-2,4-$(SiMe_3)_2$-2,4-$C_2B_4H_4$]$_4$(μ-Cl)$_2$(μ_4-O)}·(THF) (4). This compound was prepared as a white powder from the reaction of *closo-exo*-5,6-Na(THF)$_2$-1-Na(THF)$_2$-2,4-$(SiMe_3)_2$-2,4-$C_2B_4H_4$ (**1**; 1.34 g, 2.38 mmol), anhydrous $GdCl_3$ (0.50 g, 1.90 mmol), and H_2O (0.0086 g, 0.48 mmol) in a molar ratio of 5:4:1 in 30 mL of dry THF by using a procedure similar to that described in the synthesis of **2**. Yield: 0.66 g, 0.40 mmol (84%). Anal. Calcd (found) for $C_{32}H_{88}B_{16}Cl_2Gd_4OSi_8$·THF: C, 26.07 (26.34); H, 5.83 (5.75). IR (cm^{-1}, KBr pellet): 2956 (s), 2889 (m), 2532 (br, s) [ν(B−H)], 1398 (s), 1240 (s), 1178 (m) 1140 (m), 1024(s), 842 (vs), 753 (m), 687 (m), 629 (m). No useful NMR spectra could be obtained.

Synthesis of {[η^5-1-Tb(THF)-2,4-$(SiMe_3)_2$-2,4-$C_2B_4H_4$]$_4$-(μ-Cl)$_2$(μ_4-O)} (5). This compound was prepared as colorless crystals from the reaction of *closo-exo*-5,6-Na(THF)$_2$-1-Na(THF)$_2$-2,4-$(SiMe_3)_2$-2,4-$C_2B_4H_4$ (**1**; 1.34 g, 2.35 mmol), anhydrous $TbCl_3$ (0.50 g, 1.88 mmol), and H_2O (0.0085 g, 0.47 mmol) in a molar ratio of 5:4:1 in 30 mL of dry THF by following a procedure similar to that used in the synthesis of **2**, except that the powdered product was further recrystallized in anhydrous benzene. Yield: 0.65 g, 0.35 mmol (73%). Anal. Calcd (found) for $C_{48}H_{120}B_{16}Cl_2Tb_4O_5Si_8$: C, 30.64 (30.89); H, 6.43 (6.63). IR (cm^{-1}, KBr pellet): 2957 (s), 2887 (m), 2533 (m) [ν(B−H)], 2497 (s, s) [ν(B−H)], 2432 (s, s) [ν(B−H)], 2386 (s, w) [ν(B−H)], 1399 (s), 1241 (s), 1179 (w), 1140 (w), 1113 (w), 1024 (s), 831 (vs), 786 (m), 691 (m), 631 (m). No useful NMR spectra could be obtained.

Synthesis of {[η^5-1-Ho-2,4-$(SiMe_3)_2$-2,4-$C_2B_4H_4$]$_4$(μ-Cl)$_2$(μ_4-O)}·THF (6). Compound **6** was obtained as yellow crystals from the reaction of *closo-exo*-5,6-Na(THF)$_2$-1-Na(THF)$_2$-2,4-$(SiMe_3)_2$-2,4-$C_2B_4H_4$ (**1**; 1.34 g, 2.35 mmol), anhydrous $HoCl_3$ (0.50 g, 1.88 mmol), and H_2O (0.0085 g, 0.47 mmol) in a molar ratio of 5:4:1 in 30 mL of dry THF by using a procedure identical with that described above for **2**. Yield: 0.65 g, 0.35 mmol (73%). Anal. Calcd (found) for $C_{32}H_{88}B_{16}Cl_2Ho_4OSi_8$·THF: C, 25.59 (25.40); H, 5.73 (5.61). IR (cm^{-1}, KBr pellet): 2952 (s), 2893 (m), 2554 (s), 2535 (w), 2526 (s), 2499 (s), 2483 (w), 2435 (sh), 2375 (s) [ν(B−H)], 1449 (s), 1399 (s), 1240 (s), 1173 (s), 1115 (m), 1072 (s), 1047 (s), 1025 (s), 934 (m), 894 (vs), 836 (m), 755 (m), 684 (m), 629 (m). No useful NMR spectra could be obtained.

Synthesis of {[η^5-1-Lu(THF)-2,4-$(SiMe_3)_2$-2,4-$C_2B_4H_4$]$_4$-(μ-Cl)$_2$(μ_4-O)} (7). The lutetacarborane **7** was prepared as colorless crystals from the reaction of *closo-exo*-5,6-Na(THF)$_2$-1-Na(THF)$_2$-2,4-$(SiMe_3)_2$-2,4-$C_2B_4H_4$ (**1**; 1.25 g, 2.22 mmol), anhydrous $LuCl_3$ (0.50 g, 1.78 mmol), and H_2O (0.0080 g, 0.45 mmol) in a molar ratio of 5:4:1 in 30 mL of dry THF by using a procedure similar to that applied in the synthesis of **2**, except that the powdered product was further recrystallized in anhydrous benzene. Yield: 0.67 g, 0.35 mmol (78%). Anal. Calcd (found) for $C_{48}H_{120}B_{16}Cl_2Lu_4O_5Si_8$: C, 29.63 (29.46); H, 6.22 (6.34). IR (cm^{-1}, KBr pellet): 2945 (s), 2918 (s), 2852 (s), 2575 (s), 2539 (m), 2510 (m), 2470 (m), [ν(B−H)], 1455 (s), 1402 (s), 1248 (s), 1109 (m), 1023 (m), 838 (vs), 691 (m), 622 (m), 543 (m). NMR data for compound **7**: ^{1}H NMR (d_8-THF, external Me_4Si) δ 0.11 [36H, s, −Si(CH_3)$_3$], 0.24 [36H, s, −Si-(CH_3)$_3$], 1.75 [16H, m, THF, $J(^1H-^1H)$ = 20 Hz], 3.60 [16H,

(22) (a) van Lenthe, E.; Baerends, E. J.; Snijders, J. G. *J. Chem. Phys.* **1993**, *99*, 4597−4610. (b) van Lenthe, E. The ZORA Equation. Thesis, Vrije Universiteit Amsterdam, Amsterdam, The Netherlands, 1996.

(23) Kohout, M. DGRID/BASIN, Version 2.4; 2002.

(24) (a) Williams, T.; Kelley, C.; et al. GNUPLOT, version 3.8k, Patchlevel 2; 2003. (b) Moore, B. G. *J. Chem. Educ.* **2000**, *77*, 785−789.

Table 1. Crystallographic Data[a] for Complexes 3 and 5−7

	3	5	6	7
formula	$C_{48}H_{120}B_{16}Cl_2Nd_4O_5Si_8$	$C_{48}H_{120}B_{16}Cl_2Tb_4O_5Si_8$	$C_{56}H_{136}B_{16}Cl_2Ho_4O_7Si_8$	$C_{48}H_{120}B_{16}Cl_2Lu_4O_5Si_8$
fw	1822.98	1881.70	2049.95	1945.90
cryst syst	monoclinic	monoclinic	monoclinic	monoclinic
space group	*C*2/*c*	*C*2/*c*	*C*2/*c*	*C*2/*c*
a, Å	23.748(5)	23.577(5)	28.403(5)	23.544(5)
b, Å	18.632(5)	18.513(5)	12.835(2)	18.440(5)
c, Å	22.798(5)	22.602(5)	27.879(5)	22.480(5)
α, deg	90.000(5)	90.000(5)	90.000	90.000(5)
β, deg	104.338(5)	104.092(5)	117.820(3)	104.153(5)
γ, deg	90.000(5)	90.000(5)	90.000	90.000(5)
V, Å^3	9774(4)	9568(4)	8989(3)	9464(4)
Z	4	4	4	4
D_{calcd}, g cm^{-3}	1.239	1.306	1.515	1.366
abs coeff, mm^{-1}	2.273	3.107	3.689	4.325
cryst dimens, mm	0.50 × 0.38 × 0.038	1.02 × 0.38 × 0.38	0.20 × 0.14 × 0.08	0.42 × 0.24 × 0.14
θ (min, max), deg	1.41, 23.00	1.42, 25.00	1.62, 25.00	1.42, 24.00
T, K	203(2)	203(2)	173(2)	203(2)
no. of data collected	16 772	17 209	17 492	25 733
no. of obsd rflns, $I > 2\sigma(I)$	6426	7414	7732	7170
no. of params refined	437	437	490	437
GOF	1.401	1.305	1.446	1.498
R1[b]	0.0795	0.0703	0.0367	0.0904
wR2[b]	0.1793	0.1686	0.0794	0.1844

[a] Graphite-monochromated Mo Kα radiation, $\lambda = 0.710\ 73$ Å. [b] $R1 = \sum||F_o| - |F_c||/\sum|F_o|$; $wR2 = [\sum w(F_o^2 - F_c^2)^2/\sum w(F_o^2)^2]^{1/2}$, $w = 1/[\sigma^2(F_o) + g(F_o)^2]$.

m, THF, $J(^1H-^1H) = 20$ Hz]; ^{13}C NMR (d_8-THF, external Me_4-Si) δ −0.39 [Si−(CH_3)$_3$], −0.01 [Si−(CH_3)$_3$], 22.77 [C_4H_8O], 64.53 [C_4H_8O], 99.89 [Si-$C_{(cage)}$]; ^{11}B NMR (d_8-THF, relative to external BF_3·OEt_2) δ 18.68 (br), 2.02 [br, basal *B*H], −33.72 [br], −51.91 [d, apical *B*H, $^1J(^{11}B-^1H) = 158$ Hz].

X-ray Analyses of 3 and 5−7. X-ray-quality crystals of **3** and **5−7** were grown from a hot benzene/THF solution by slow cooling. The crystals were mounted on a Bruker SMART CCD PLATFORM diffractometer, under a low-temperature nitrogen stream. The pertinent crystallographic data for **3** and **5−7** are summarized in Table 1. Compounds **3** and **5−7** were found to be isostructural, and the space group for all compounds was uniquely determined from systematic absences as *C*2/*c*. Intensity data were collected at 173 K. For each compound, three standard reflections were monitored during the data collection that did not show any significant change in intensities. All data, considered as observed ($I > 2\sigma(I)$), were corrected for Lorentz, polarization, and absorption effects (G. M. Sheldrick, SADABS, Program for Empirical Absorption Correction of Area Detector Data, University of Göttingen Göttingen, Germany, 1996). Semiempirical absorption studies (ψ scans) were applied for each structure, and the relevant minimum and maximum transmission factors are listed in Table 1. All structures were solved by direct methods and refined by full-matrix least-squares techniques using the SHELXTL system of programs.[25] All structures were refined on F^2 for all reflections.[26] The weighted value R_w and goodness of fit were based on F^2. The observed criterion of $F > 4.0\sigma(F)$ was used only for the *R* factor calculation; it was not relevant to the choice of reflections for refinement. For **6**, two nonsolvating THF molecules located at the interval of the structure were present in each molecular structure. Full-matrix refinement was performed for each structure. In all of the structures, the non-H atoms were refined anisotropically. The noncoordinated THF's were disordered and were elastically restrained in the final stages of refinement. The carborane-cage H atoms of **3** and **5−7** were located in ΔF maps. The final values of *R* and weighted R_w are listed in Table 1. For all structures $R = \sum||F_o| - |F_c||/\sum|F_o|$ and $R_w = [\sum w(F_o^2 - F_c^2)^2/\sum w(F_o^2)^2]]^{1/2}$ ($w = [\sigma^2(F) + 0.001(F)^2]^{-1}$). Some selected interatomic distances and angles are listed in Tables 2 and 3, respectively. The detailed crystallographic parameters of all compounds can be found in the Supporting Information.

(25) Sheldrick, G. M. SHELXTL, Version 5.1; Bruker Analytical X-ray Systems, Madison, WI, 1997.
(26) Sheldrick, G. M. SHELXTL93, Program for the Refinement of Crystal Structures; University of Göttingen, Göttingen, Germany, 1993.

Results and Discussion

Synthesis. Anhydrous $LnCl_3$ (Ln = La, Nd, Gd, Tb, Ho, Lu) was treated with a stoichiometric quantity of freshly distilled H_2O under reflux conditions in THF (see Experimental Section). The resulting mixtures were then reacted with *closo-exo*-5,6-Na(THF)$_2$-1-Na(THF)$_2$-2,4-($SiMe_3$)$_2$-2,4-$C_2B_4H_4$ (**1**) in an overall **1**:$LnCl_3$:H_2O molar ratio of 5:4:1 at −78 °C. Refluxing of this mixture overnight gave microcrystalline or powdered solids of the new oxolanthanacarboranes {[η^5-1-Ln(THF)$_n$-2,4-($SiMe_3$)$_2$-2,4-$C_2B_4H_4$]$_4$(μ-Cl)$_2$(μ_4−O)}·*y*THF (Ln = La (**2**), *n* = 0, *y* = 1; Nd (**3**), *n* = 1, *y* = 0; Gd (**4**), *n* = 0, *y* = 1; Tb (**5**), *n* = 1, *y* = 0; Ho (**6**), *n* = 0, *y* = 1; Lu (**7**), *n* = 1, *y* = 0) in 75, 78, 84, 73, 86, and 78% yields, respectively. When these reaction products were recrystallized from hot benzene/THF solutions, X-ray-quality crystals of **3** and **5−7** were isolated. The X-ray samples of **2**, **4**, and **6** differ in formula from those given above, in that all show that each metal is coordinated by a THF molecule, whereas the analytical samples, which were vacuum-dried, do not show such coordination. It is assumed that the coordinating THF molecules do not materially change the Ln_4O core structure. A general synthetic procedure is outlined in Scheme 1. It is important to note that the $LnCl_3/H_2O$/THF mixture must be refluxed until a homogeneous solution is obtained. If $LnCl_3$ and H_2O were added to a solution of **1** without prior refluxing, the water directly attacked and rapidly decomposed the carborane ligand. The oxolanthanacarboranes were obtained in good yields only when the reactions were carried out first at −78 °C and then completed at reflux temperatures. Although oxygen coordination numbers ranging from 3 to 6 have been observed for f-block metal complexes,[4,6b] there does not

Table 2. Selected Bond Lengths (Å) for 3 and 5−7

			Compound **3**				
Nd(1)−O	2.369(7)	O−Nd(1)#1	2.369(7)	Nd(1)−B(24)#1	2.878(16)	Nd(2)−B(14)	2.861(15)
Nd(1)−O(31)	2.499(10)	O−Nd(2)#1	2.378(7)	Nd(1)−B(25)#1	2.770(16)	Nd(2)−B(15)	2.763(15)
Nd(1)−Cl(2)	2.798(3)	Nd(1)−B(12)	2.787 (17)	Nd(2)−C(21)	2.794(13)	B(24)−Nd(1)#1	2.878(16)
Nd(2)−Cl(1)	2.781(3)	Nd(1)−B(14)	2.752(17)	Nd(2)−B(22)	2.766(16)	B(25)−Nd(1)#1	2.770(16)
Nd(2)−Nd(1)#1	3.825(1)	Nd(1)−B(15)	2.757(17)	Nd(2)−C(23)	2.779(13)	Nd(1)−Cnt(1)	2.433
Cl(1)−Nd(2)#1	2.781(3)	Nd(1)−C(13)	2.790(13)	Nd(2)−B(24)	2.767(14)	Nd(2)−Cnt(2)	2.433
Cl(2)−Nd(1)#1	2.798(3)	Nd(1)−C(11)	2.801(14)	Nd(2)−B(25)	2.785(16)		
			Compound **5**				
Tb(1)−O	2.299(5)	O−Tb(1)#1	2.299(5)	Tb(1)−B(24)#1	2.847(14)	Tb(2)−B(14)	2.825 (13)
Tb(1)−O(31)	2.423(9)	O−Tb(2)#1	2.313(5)	Tb(1)−B(25)#1	2.762(13)	Tb(2)−B(15)	2.695(14)
Tb(1)−Cl(2)	2.727(3)	Tb(1)−B(12)	2.732 (13)	Tb(2)−C(21)	2.705(12)	B(24)−Tb(1)#1	2.847(14)
Tb(2)−Cl(1)	2.715(3)	Tb(1)−B(14)	2.685(13)	Tb(2)−B(22)	2.750(13)	B(25)−Tb(1)#1	2.726(13)
Tb(2)−Tb(1)#1	3.7041(9)	Tb(1)−B(15)	2.696(14)	Tb(2)−C(23)	2.728(11)	Tb(1)−Cnt(1)	2.358
Cl(1)−Tb(2)#1	2.715(3)	Tb(1)−C(13)	2.732(12)	Tb(2)−B(24)	2.697(13)	Tb(2)−Cnt(2)	2.359
Cl(2)−Tb(1)#1	2.727(3)	Tb(1)−C(11)	2.720(11)	Tb(2)−B(25)	2.704(15)		
			Compound **6**				
Ho(1)−O	2.282(3)	O−Ho(2)#1	2.284(3)	Ho(1)−B(24)#1	2.756(7)	Ho(2)−B(15)	2.676(7)
Ho(1)−O(31)	2.397(4)	Cl(1)−Ho(1)#1	2.706(1)	Ho(1)−B(25)#1	2.679(7)	B(24)−Ho(1)#1	2.756(7)
Ho(1)−Cl(1)	2.705(1)	Cl(2)−Ho(2)#1	2.708(1)	Ho(2)−C(21)	2.669(6)	B(25)−Ho(1)#1	2.679(7)
Ho(2)−O	2.284(3)	Ho(1)−B(12)	2.732 (6)	Ho(2)−B(22)	2.745(6)	Ho(1)−Cnt(1)	2.324
Ho(2)−Cl(2)	2.707(1)	Ho(1)−B(14)	2.675(7)	Ho(2)−C(23)	2.741(6)	Ho(2)−Cnt(2)	2.331
Ho(1)−Ho(2)	3.651(0)	Ho(1)−B(15)	2.630(7)	Ho(2)−B(24)	2.663(6)		
Ho(1)−Ho(2)#1	3.653(0)	Ho(1)−C(13)	2.729(6)	Ho(2)−B(25)	2.637(7)		
O−Ho(1)#1	2.282(3)	Ho(1)−C(11)	2.672(6)	Ho(2)−B(14)	2.776 (7)		
			Compound **7**				
Lu(1)−O	2.244(8)	O−Lu(1)#1	2.243(8)	Lu(1)−B(24)	2.598(18)	Lu(2)−B(14)	2.850 (19)
Lu(1)−O(31)	2.354(12)	O−Lu(2)#1	2.244(8)	Lu(1)−B(25)	2.650(20)	Lu(2)−B(15)	2.650(20)
Lu(1)−Cl(2)	2.670(4)	Lu(1)−B(12)	2.682(19)	Lu(2)−C(21)	2.630(15)	B(24)−Lu(1)#1	2.817(18)
Lu(2)−Cl(1)	2.647(4)	Lu(1)−B(14)	2.600(20)	Lu(2)−B(22)	2.670(20)	B(25)−Lu(1)#1	2.650(20)
Lu(2)−Lu(1)#1	3.5967(11)	Lu(1)−B(15)	2.620(20)	Lu(2)−C(23)	2.673(16)	Lu(1)−Cnt(1)	2.282
Cl(1)−Lu(2)#1	2.647(4)	Lu(1)−C(13)	2.650(17)	Lu(2)−B(24)	2.598(18)	Lu(2)−Cnt(2)	2.279
Cl(2)−Lu(1)#1	2.670(4)	Lu(1)−C(11)	2.671(15)	Lu(2)−B(25)	2.650 (20)		

Table 3. Selected Bond Angles (deg) for Compounds 3 and 5−7

		Compound **3**			
O−Nd(1)−O(31)	153.8(3)	O(31)−Nd(1)−Cl(2)	87.4(3)	Nd(1)−O−Nd(1)#1	114.3(5)
O−Nd(1)−B(14)	84.1(3)	O−Nd(1)−B(24)#1	82.0(3)	Nd(1)−O−Nd(2)	107.48(3)
O(31)−Nd(1)−B(14)	122.1(4)	O−Nd(1)−Nd(2)#1	36.40(12)	Nd(1)#1−O−Nd(2)	107.38(3)
O−Nd(1)−B(15)	77.2(3)	O(31)−Nd(1)−Nd(2)#1	127.1(2)	Nd(1)−O−Nd(2)#1	107.38(3)
O(31)−Nd(1)−B(15)	124.4(4)	O−Nd(1)−Nd(2)	36.35(12)	Nd(1)#1−O−Nd(2)#1	107.48(3)
O−Nd(1)−B(25)#	78.2(4)	O(31)−Nd(1)−Nd(2)	169.6(2)	Nd(2)−O−Nd(2)#1	113.0(5)
O−Nd(1)−B(12)	132.1(4)	O−Nd(2)−Nd(1)#1	36.22(12)	Cnt(1)−Nd(1)−O	104.27
O(31)−Nd(1)−B(25)#	100.1(4)	Nd(2)#−Cl(1)−Nd(2)	90.97(14)	Cnt(1)−Nd(1)−Cl	107.41
O−Nd(1)−Cl(2)	77.5(3)	Nd(1)#1−Cl(2)−Nd(2)#1	90.65(14)		
		Compound **5**			
O−Tb(1)−O(31)	152.2(2)	O(31)−Tb(1)−Cl(2)	87.3(2)	Tb(1)−O−Tb(1)#1	115.3(4)
O−Tb(1)−B(14)	85.2(3)	O−Tb(1)−B(24)#1	82.2(3)	Tb(1)−O−Tb(2)	107.12(2)
O(31)−Tb(1)−B(14)	122.4(4)	O−Tb(1)−Tb(2)#1	36.69(10)	Tb(1)#1−O−Tb(2)	106.89(2)
O−Tb(1)−B(15)	78.3(3)	O(31)−Tb(1)−Tb(2)#1	125.3(2)	Tb(1)−O−Tb(2)#1	106.89(2)
O(31)−Tb(1)−B(15)	125.2(4)	O−Tb(1)−Tb(2)	36.57(10)	Tb(1)#1−O−Tb(2)#1	107.12(2)
O−Tb(1)−B(25)#	79.0(3)	O(31)−Tb(1)−Tb(2)	171.0(2)	Tb(2)−O−Tb(2)#1	113.8(4)
O−Tb(1)−B(12)	134.6(3)	O−Tb(2)−Tb(1)#1	36.42(10)	Cnt(1)−Tb(1)−O	106.10
O(31)−Tb(1)−B(25)#	98.1(4)	Tb(2)#1−Cl(1)−Tb(2)	91.01(12)	Cnt(1)−Tb(1)−Cl	108.62
O−Tb(1)−Cl(2)	77.0(2)	Tb(1)#1−Cl(2)−Tb(1)	90.78(12)		
		Compound **6**			
O−Ho(1)−O(31)	152.49(12)	O(31)−Ho(1)−Cl(1)	87.48(10)	Ho(1)−O−Ho(1)#1	116.3(2)
O−Ho(1)−B(14)	85.10(16)	O−Ho(1)−B(24)#1	82.47(14)	Ho(1)−O−Ho(2)	106.21(2)
O(31)−Ho(1)−B(14)	122.30(18)	O−Ho(1)−Ho(2)#1	36.87(5)	Ho(1)#1−O−Ho(2)	106.31(2)
O−Ho(1)−B(15)	79.57(14)	O(31)−Ho(1)−Ho(2)#1	125.68(10)	Ho(1)−O−Ho(2)#1	106.31(2)
O(31)−Ho(1)−B(15)	124.4(4)	O−Ho(1)−Ho(2)	36.92(5)	Ho(1)#1−O−Ho(2)#1	106.21(2)
O−Ho(1)−B(25)#	98.79(17)	O(31)−Ho(1)−Ho(2)	169.91(10)	Ho(2)−O−Ho(2)#1	115.9(2)
O−Ho(1)−B(12)	136.82(15)	O−Ho(2)−Ho(1)#1	36.82(5)	Cnt(1)−Ho(1)−O	107.55
O(31)−Ho(1)−B(25)#	98.79(17)	Ho(2)#1−Cl(2)−Ho(2)	91.31(6)	Cnt(1)−Ho(1)−Cl	110.80
O−Ho(1)−Cl(1)	76.12(11)	Ho(1)#1−Cl(1)−Ho(1)#1	91.48(6)		
		Compound **7**			
O−Lu(1)−O(31)	150.4(3)	O(31)−Lu(1)−Cl(2)	86.7(3)	Lu(1)−O−Lu(1)#1	115.5(6)
O−Lu(1)−B(14)	87.3(5)	O−Lu(1)−B(24)#1	81.5(4)	Lu(1)−O−Lu(2)	106.69(3)
O(31)−Lu(1)−B(14)	121.9(5)	O−Lu(1)−Lu(2)#1	36.71(15)	Lu(1)#1−O−Lu(2)	106.56(3)
O−Lu(1)−B(15)	79.9(5)	O(31)−Lu(1)−Lu(2)#1	123.4(3)	Lu(1)−O−Lu(2)#1	106.56(3)
O(31)−Lu(1)−B(15)	125.7(6)	O−Lu(1)−Lu(2)	36.64(15)	Lu(1)#1−O−Lu(2)#1	106.69(3)
O−Lu(1)−B(25)#	80.0(5)	O(31)−Lu(1)−Lu(2)	172.7(3)	Lu(2)−O−Lu(2)#1	115.1(6)
O−Lu(1)−B(12)	137.2(4)	O−Lu(2)−Lu(1)#1	36.73(15)	Cnt(1)−Lu(1)−O	108.54
O(31)−Lu(1)−B(25)#	95.8(5)	Lu(2)#1−Cl(1)−Lu(2)	91.29(18)	Cnt(1)−Lu(1)−Cl	109.90
O−Lu(1)−Cl(2)	76.9(3)	Lu(1)#1−Cl(2)−Lu(1)#1	90.62(18)		

seem to be any consistency in either the precursor or the synthetic procedures. Clusters with a tetrahedral Ln_4O core like those of **2**−**7** were found for $[Ln_4(\mu_4\text{-}O)(NHPh)_3(OSiMe_2NPh)_6{\cdot}Na_6(THF)_7]$ (Ln = Gd, Yb), which were obtained in low yields (8.9%) from the reaction of $LnBr_3$, NaNHPh, and $(Me_2SiO)_3$ in THF,[27] while the planar Ln_4O core in $Na_6\{[(C_6H_5SiO_2)_8]_2Nd_4(\mu_4\text{-}O)\}$ was obtained in 16% yield from the reaction of anhydrous $NdCl_3$ and sodium oligo(phenylsiloxanolate) in an *n*-butanol solution.[28a] The planar Ln_4O core cluster in

Scheme 1. Syntheses of an Oxide Ion Encapsulating Tetralanthanide Tetrahedra Surrounded by "Carbons-Apart" 2,4-$C_2B_4H_4$ Carborane Cages

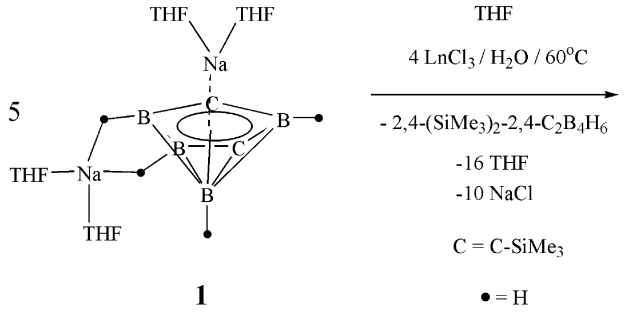

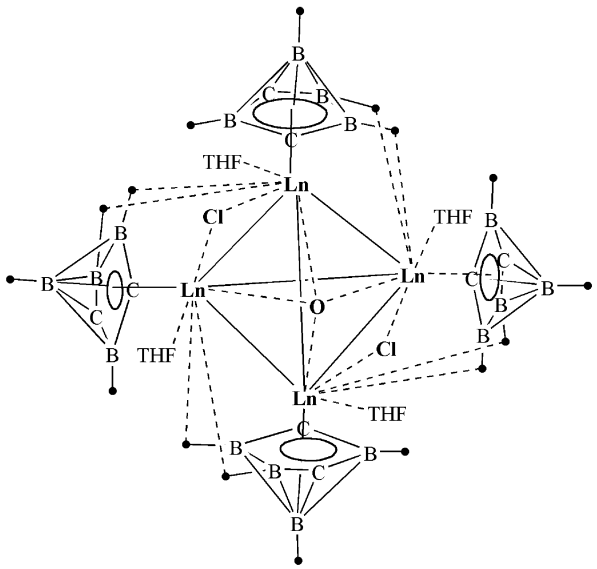

Ln = La (**2**), Nd (**3**), Gd (**4**), Tb (**5**), Ho (**6**) and Lu (**7**)

$[Tb_4L_2(NO_3)_4(MeOH)_2(\mu_4\text{-O})]$ (H_3L = 1,3-bis((2-hydroxy-3-methoxybenzyl)amino)propan-2-ol) was obtained by the reaction of hydrated $Tb(NO_3)_3{\cdot}5H_2O$ with H_3L in a 2:1 ratio in methanol.[28b] On the other hand, the butterfly form of Ce_4O in the cerium complex $Ce_4O(O^iPr)_{13}(^iPrOH)$ was obtained from the photoreduction of $Ce_2(O^i\text{-}Pr)_8(^iPrOH)$ in a 2:1 mixture of $MeOC_2H_4OMe$ and *i*-PrOH.[6b] The complexity is illustrated by the report of Evans and co-workers on the reactions of YCl_3 and $LaCl_3$ with $NaOCMe_3$ under different conditions.[4] While a 1:3 molar reaction of YCl_3 and $NaOCMe_3$ in THF produced the trinuclear $Y_3(\mu_3\text{-}OCMe_3)(\mu_3\text{-}Cl)(\mu\text{-}OCMe_3)\text{-}(OCMe_3)_4(THF)_2$, in which the metals form a triangular core, the same reaction, when carried out in the presence of Me_3COH, produced an isomeric compound differing in the placement of the two THF molecules. The reaction of $LaCl_3$ with 3 equiv of $NaOCMe_3$ in THF produced the compound $La_3(\mu_3\text{-}OCMe_3)_2(\mu\text{-}OCMe_3)\text{-}(OCMe_3)_4(THF)_2$, which is similar to the trinuclear Y complex, except that $OCMe_3$ now occupies both triply bridging positions. On the other hand, the 1:2 molar ratio reaction of YCl_3 and $LiOCMe_3$ produced the dimer $[Y_4(\mu_3\text{-}OCMe_3)(\mu\text{-}OCMe_3)_4(OCMe_3)_4(\mu_4\text{-O})(\mu\text{-Cl})_2Li_4(\mu\text{-}OCMe_3)_2]_2$, in which the Y_4 cores are arranged in a butterfly arrangement about an oxide ion. Somewhat similar complexity is found for the lanthanacarboranes. We have previously shown that the reaction of *closo-exo*-5,6-Li(THF)$_2$-1-Li(THF)$_2$-2,3-$(SiMe_3)_2$-2,3-$C_2B_4H_4$ with $LnCl_3$ in a 2:1 molar ratio at room temperature gave, exclusively, the trinuclear clusters of the half-sandwich lanthanacarboranes $\{[\eta^5\text{-1-Ln-2,3-}(SiMe_3)_2\text{-2,3-}C_2B_4H_4]_3[(\mu\text{-1-Li-2,3-}(SiMe_3)_2\text{-2,3-}C_2B_4H_4)_3\text{-}(\mu_3\text{-OMe})][\mu\text{-Li(THF)}]_3(\mu_3\text{-O})\}$ (Ln = Nd, Sm, Gd, Tb, Dy Ho), presumably through the reaction of THF degradation products with an initially formed half-sandwich lanthanacarborane.[8] The uncontrolled stoichiometry makes it impossible to assess the driving forces in these reactions. However, the products are not due to the adventitious presence of water. The "carbons apart" carborane (2,4-C_2B_4) does not seem to be conducive to fostering a similar THF decomposition.[11] However, our present work, shown in Scheme 1, shows that in the presence of an available source for the oxide ion (through H_2O) the encapsulated compounds **2**−**7** readily form. As best as we can determine, the product formulations of **2**−**7** are dictated by the inherent stabilities of the complexes. The best yields were obtained from "exact" stoichiometric mixtures, assuming one carborane dianion acts as a proton scavenger; there is NMR evidence for the formation of a neutral *nido*-carborane in the final reaction mixture. A 1:1 carborane:Ln molar ratio led to the same products, but in lower yields. In addition, reactions in which the Ln:H_2O ratios were less than 4:1 resulted in the formation of inseparable product mixtures, while higher ratios produced the tetralanthanide clusters **2**−**7** and the unreacted carborane precursor.

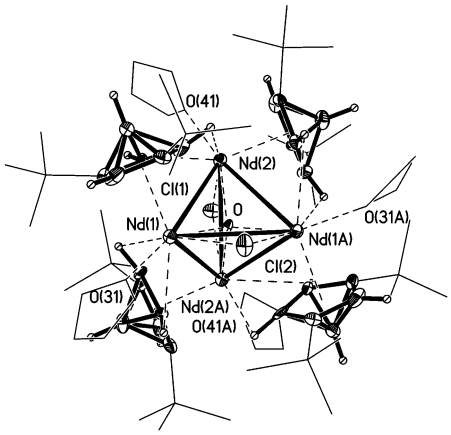

Figure 1. Perspective view of the oxide ion encapsulating tetrahedron with each corner connecting to a *closo*-neodymacarborane complex (**3**). Thermal ellipsoids are drawn at the 50% probability level. The coordinated THF molecules and the *exo*-polyhedral $SiMe_3$ groups are drawn with thin lines.

Crystal Structures. The structures of compounds **3** and **5**−**7** are shown in Figures 1−4, respectively. As usual, the lines between atoms show only connectivity and do not necessarily denote covalent bonds. Table 2 lists some important bond distances, and Table 3 gives some selected bond angles. Complexes **3**, **5**, and **7** are isostructural; two additional uncoordinated THF mol-

(27) Kraut, S.; Magull, J.; Schaller, U.; Karl, M.; Harms, K.; Dehnicke, K. *Z. Anorg. Allg. Chem.* **1998**, *624*, 1193−1201.

(28) (a) Shchegolikhina, O. I.; Pozdniakova, Y. A.; Lindeman, S. V.; Zhdanov, A. A.; Psaro, R.; Ugo, R.; Gavioli, G.; Battisuzzi, R.; Borsari, M.; Rüffer, T.; Zhcchi, C.; Pályi, G. *J. Organomet. Chem.* **1996**, *514*, 29−35. (b) Lam, A. W.-H.; Wong, W.-T.; Wen. G.; Zhang, X.-X.; Gao, S. *New J. Chem.* **2001**, *25*, 531−533.

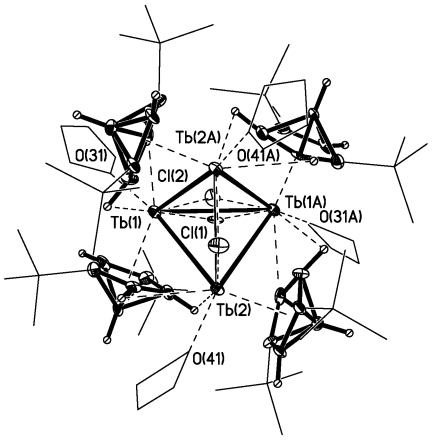

Figure 2. Perspective view of the oxide ion encapsulating tetrahedron with each vertex connecting to a *closo*-terbacarborane complex (**5**). Thermal ellipsoids are drawn at the 50% probability level. The coordinated THF molecules and the exo-polyhedral $SiMe_3$ groups are drawn with thin lines.

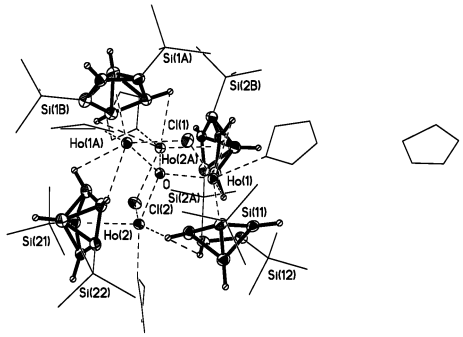

Figure 3. Perspective view of the oxide ion encapsulating tetrahedron with each corner connecting to a *closo*-holmacarborane complex (**6**). Thermal ellipsoids are drawn at the 50% probability level. The coordinated, as well as the noncoordinated, THF molecules and the exo-polyhedral $SiMe_3$ groups are drawn with thin lines.

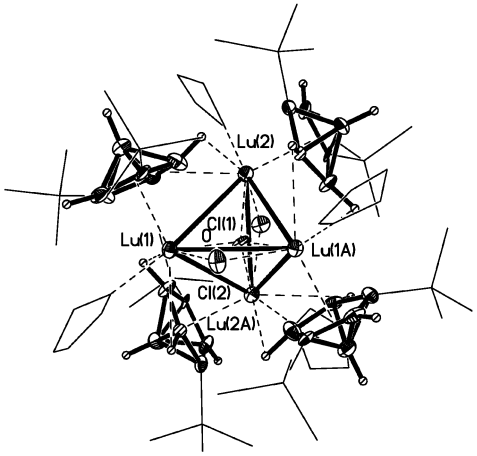

Figure 4. Perspective view of the oxide ion encapsulating tetrahedron with each vertex connecting to a *closo*-lutetacarborane complex (**7**). Thermal ellipsoids are drawn at the 50% probability level. The coordinated THF molecules and the exo-polyhedral $SiMe_3$ groups are drawn with thin lines.

ecules are found in the unit cell of compound **6**. In all of the structures, each lanthanide metal atom is coordinated by a C_2B_4 cage and, via two Ln−H−B bridges, by a neighboring C_2B_4 cage. The O−metal distances are 2.369 ± 0.007, 2.299 ± 0.005, 2.283 ± 0.001, and 2.244 ± 0.008 Å for **3** and **5**−**7**, respectively. The metal−oxygen−metal bond angles are as follows for **3** (Ln = Nd), **5** (Ln = Tb), **6** (Ln = Ho) and **7** (Ln = Lu), respectively: Ln(1)−O−Ln(2) = 107.48(3), 107.12(2), 106.21(2), 106.69(3); Ln(1)−O−Ln(1A) = 114.3(5), 115.3-(4), 116.2(2), 115.5(6); Ln(1)−O−Ln(2A) = 107.38(3), 106.89(2), 106.31(2), 106.56(3)° . These angles suggest a slightly distorted tetrahedral arrangement of the metals around the oxide oxygen. Each of the lanthanide metals is associated with an η^5-bonded C_2B_4 cage, with average Ln−cage centroid distances of 2.433, 2.358, 2.328, and 2.280 Å for **3** and **5**−**7**, respectively. These Ln−cage centroid distances are quite close to those found in the lanthanide complexes of both the "carbons adjacent" and "carbons apart" C_2B_4-carborane ligand systems.[8,10,11,30] Figures 1−4 show that each diagonal pair of Ln metals is linked by a bridging chloride to give the $[(C_2B_4Ln)_4Cl_2O]$ core. Table 2 shows that both the Ln−O and the Ln−Cnt bond distances decrease in the order Nd > Tb > Ho > Lu, which is the same order as the decrease in the ionic radii of the Ln^{3+} ions,[31] suggesting an essentially ionic metal−ligand interaction. This same trend has been noted in the corresponding trinuclear Ln−carborane complexes,[8] in lanthanacarboranes containing two or three carborane cages,[11,30] and in the lanthanocenes.[32] The ionic nature of the bonding is also seen in the DFT results on the model compound $La_4OCl_2(2,4\text{-}C_2B_4H_6)_4(OH_2)_4$. Figure 5 shows a plot of the electron localization function[33,34] (ELF) in

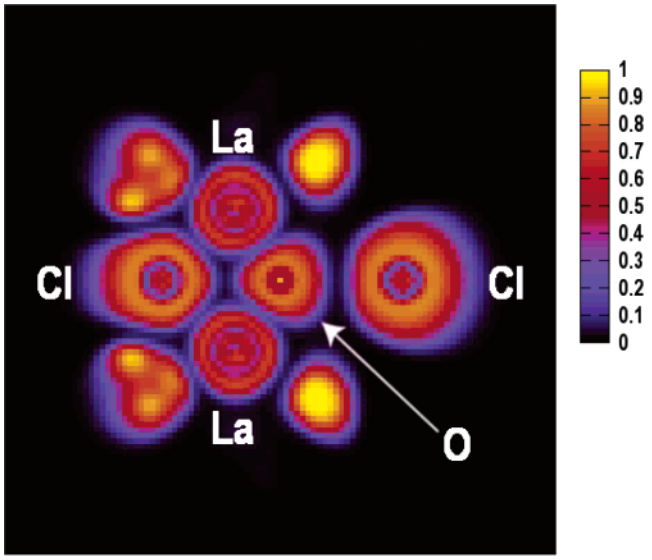

Figure 5. Plot of the electron localization function (ELF) for a slice through the $La_4OCl_2(C_2B_4H_6)_4(OH_2)_4$ molecule in a plane containing the central oxygen, two of the lanthanum centers, and the two Cl atoms.

(29) Kahn, O. *Molecular Magnetism*; VCH: New York, 1993. Boundreaux, E. A.; Mulay, L. N. *Theory and Applications of Molecular Paramangetism*; Wiley: New York, 1976.
(30) Wang, J.; Li, S.; Zheng, C.; Maguire, J. A.; Sarkar, B.; Kaim, W.; Hosmane, N. S. *Orgnometallics* **2003**, *22*, 4334.
(31) Shannon, R. D. *Acta Crystallogr., Sect. A* **1976**, *32*, 751.
(32) Savin, A.; Jepsen, O.; Flad, J.; Andersen, O. K.; Preuss, H.; von Schnering, H. G. *Angew. Chem.* **1992**, *104*, 186−188 (see also *Angew. Chem., Int. Ed. Engl.* **1992**, *31*, 187−188).
(33) Becke, A. D.; Edgecombe, K. E. *J. Chem. Phys.* **1990**, *92*, 5397−5403.
(34) Binder, H.; Kellner, R.; Vaas, K.; Hein, M.; Baumann, F.; Wanner, M.; Kaim, W.; Wedig, U.; Hönle, W.; von Schering, H. G.; Groeger, O.; Engelhardt, G. *Z. Anorg. Allg. Chem.* **1999**, *625*, 1638−1646.

a plane passing through the core and containing the O, two La atoms, and the two Cl atoms. Values of the ELF close to zero appear at the midpoint along the $La^{3+}\cdots O^{2-}$ and $La^{3+}\cdots Cl^{-}$ internuclear axes, as is typical for ionic bonds. In contrast to this, a plot of the ELF for the same $La_4OCl_2(C_2B_4H_6)_4(OH_2)_4$ cluster system in a plane that contains one of the five-membered C_2B_3 rings shows ELF values close to 1 at the C−B and B−B bond midpoints. The ELF has been used previously to provide a graphical portrayal of the bonding in borane clusters.[35] The average metal−metal distances are 3.826 ± 0.001, 3.707 ± 0.001, 3.653 ± 0.001, and 3.598 ± 0.001 Å for compounds **3** and **5**−**7**, respectively. Such long distances indicate that there are no direct metal−metal interactions between the metals in all of these structures, which can also be inferred from Figure 5. In addition, the lack of 4f electrons in the calculated cluster, together with the model's close structural similarity to the experimentally determined cluster structures, suggests that the presence of f electrons in the latter has a negligible effect on cluster structure. That is to say, metal−metal bonding need not be invoked to explain the structure of any of the clusters considered here.

Spectra. Compounds **2**−**7** were characterized by IR spectroscopy and elemental analyses. The analytical samples for compounds **2**, **4**, and **6** were taken from the powdered products directly after purification and high-vacuum drying. Therefore, these samples contained only one THF molecule per tetrameric unit. This is different from the samples used for crystal structure analyses, which show each metal coordinated to a THF molecule. Consequently, the microanalytical data for **3**, **5**, and **7** show results consistent with the crystal structures. The IR spectra of the lanthanacarboranes all exhibit well-resolved multiple terminal B−H stretching vibrations in the 2270−2590 cm^{-1} range. Such fine structures of B−H stretching bands have been previously observed in other *closo*- and *commo*-lanthanacarboranes and lithiacarboranes. They have been explained on the basis of unequal interactions of the boron-bound hydrogen atoms with metal groups present in the complex.[8−11,30] Because of the strong paramagnetism of the complexes **3**−**6**, no useful NMR spectra could be obtained. However, the diamagnetic lanthanum and lutetium complexes **2** and **7** were found to provide interpretable NMR spectral data. In both compounds the ^1H NMR spectra showed two multiplets at δ 3.58, 1.73 ppm (for **2**), and 3.60, 1.75 ppm (for **7**), respectively, which are due to the CH_2 groups in THF. Two singlets at δ 0.01, 0.18 ppm (for **2**) and δ 0.11, 0.24 ppm (for **7**) are assigned to the CH_3 protons of the $SiMe_3$ groups. The ^{13}C NMR spectra show the presence of the cage carbon atoms and the THF molecules, plus two peaks due to CH_3 carbon atoms of the $SiMe_3$ groups at δ 2.19, 0.294 ppm (for **2**) and δ 0.01, −0.39 ppm (for **7**), respectively. The two resonances for the $SiMe_3$ hydrogen and carbon atoms indicate two different chemical environments for the trimethylsilyl groups. This is consistent with the ^{11}B NMR spectra, which show four peaks in a 1:1:1:1 peak area ratio. The chemical shifts found for **2** were at δ 23.07, 1.98, −33.94, and −52.21 ppm and for **7** at δ 18.68, 2.02, −33.72, and −51.91 ppm. These peak area patterns are very different from that of the precursor *closo-exo*-5,6-$Na(THF)_2$-1-$Na(THF)_2$-2,4-$(SiMe_3)_2$-2,4-$C_2B_4H_4$, which shows a set of three doublets at δ 16.3, 5.4, and −54.2 ppm in a 1:2:1 peak area ratio,[14] and also from that of the full-sandwich species 2,2′,4,4′-$(SiMe_3)_4$-3,5′,6′-[(μ-H)$_3$Na((THF)$_2$}]-1,1′-*commo*-Lu(η^5-2,4-$C_2B_4H_4)_2$, which has resonances at δ 28.5, 7.0, and −47.3 ppm in a similar 1:2:1 peak area ratio.[30] These resonances have been assigned to the unique boron (1B), the basal boron (2B), and the apical boron atoms (1B), respectively. In general, the apical boron resonance is shaped such that the splitting due to its terminal hydrogen can be easily resolved. Therefore, the upfield resonances at δ −52.21 and −51.91 ppm for compounds **2** and **7**, respectively, can be assigned to the apical boron atoms and the most downfield peaks (δ 23.07 (**2**) and 18.86 (**7**) ppm) to the unique boron atoms. These assignments indicate that one of the two adjacent basal boron atoms becomes significantly more shielded on forming the tetranuclear cluster. Reference to Figure 4 and Table 2 shows that each Lu is η^5 bonded by one carborane cage and also interacts significantly with one of the basal boron atoms of a neighboring carborane cage; for example, the Lu(1)−B(15) distance is 2.620(20) Å, which is essentially the same as the 2.650(20) Å value found for the Lu(2)−B(15) distance. Therefore, from the structure shown in Figure 4 one would expect nonequivalency of the C_2B_4 cage atoms, although the chemical shift effects arising from different basal boron environments are surprising. It should also be pointed out that the solution structure of **7** may be different from that shown in Figure 4. At this point all that can be noted is that the solution spectral data of **7** are in qualitative agreement with the solid-state structure.

Magnetic Susceptibility. The molar magnetic susceptibility of compound **6**, measured between 5 K and room temperature, follows the Curie−Weiss law, $\chi = C/(T - \Theta)$ with Θ being equal to virtually 0 K, indicating negligible magnetic interaction between the metals. The Curie constant, *C*, corresponds to an effective magnetic moment of 10.3 μ_B per Ho atom for **6**, which is very close to the value of 10.6 μ_B for the free Ho^{3+} ion ($^5I_8$ ground state).[36] These results are similar to those found for other lanthanacarboranes and indicate that crystal field effects play little or no role in the temperature range studied.[10,30]

Conclusions. The reactions of *closo-exo*-5,6-$Na(THF)_2$-1-$Na(THF)_2$-2,4-$(SiMe_3)_2$-2,4-$C_2B_4H_4$ (**1**) with a number of $LnCl_3$ compounds and H_2O in molar ratios of 5:4:1 produced the novel oxide ion encapsulating tetralanthanacarborane cluster complexes {[η^5-1-Ln$(THF)_n$-2,4-$(SiMe_3)_2$-2,4-$C_2B_4H_4]_4(\mu$-$Cl)_2(\mu_4$-O)}·*y*THF in consistently high yields. Variation in the stoichiometric molar ratios failed to produce any other lanthanacarborane complexes. Thus, the present work demonstrates the systematic synthetic approach of using water as one of the controlled reagents to construct hitherto unexplored lanthanacarborane clusters comprising a $[(C_2B_4Ln)_4Cl_2O]$

(35) (a) Schumann, H.; Genthe, W.; Bruncks, N. *Angew. Chem.* **1981**, *93*, 126; *Angew. Chem., Int. Ed. Engl.* **1981**, *20*, 119. (b) Schumann, H.; Genthe, W.; Bruncks, N.; Pickardt, J. *Organometallics* **1982**, *1*, 1194. (c) Maginn, R. W.; Manastyrskj, S.; Dudeck, M. *J. Am. Chem. Soc.* **1963**, *85*, 672. (d) Evans, W. J.; Wayda, A. L.; Hunter, W. E.; Atwood, J. L. *J. Chem. Soc., Chem. Commun.* **1981**, 292−293.

(36) (a) Van Vleck, J. H.; Frank, N. *Phys. Rev.* **1929**, *34*, 1494. (b) Yost, D. M.; Russell, H., Jr.; Garner, C. S. *The Rare Earth Elements and Their Compounds*; Wiley: New York, 1947; p 14.

core. Reactivity studies of these clusters toward a variety of organic substrates in both the aqueous and organic media are currently underway in our laboratories.

Acknowledgment. This work was supported by grants from the National Science Foundation (Grant No. CHE-0241319), the donors of the Petroleum Research Fund, administered by the American Chemical Society, The Robert A. Welch Foundation (Grant No. N-1322 to J.A.M.) and Northern Illinois University through a Presidential Research Professorship. N.S.H. and C.C.C. gratefully acknowledge the Forschungspreis der Alexander von Humboldt-Stiftung.

Supporting Information Available: Tables of crystallographic data as CIF files, including fractional coordinates, bond lengths and angles, anisotropic displacement parameters, and hydrogen atom coordinates, of **3** and **5**−**7**, along with selected interatomic distances for the calculated structure of $La_4OCl_2(C_2B_4H_6)_4(OH_2)_4$. This material is available free of charge via the Internet at http://pubs.acs.org.

OM0496176